PNAS

Supplementary Information for

IGF1 Receptor Regulates Upward Firing Rate Homeostasis via the Mitochondrial Calcium Uniporter

Maxim Katsenelson, Ilana Shapira, Eman Abbas, Kristina Jevdokimenko, Boaz Styr, Antonella Ruggiero, Saba Aïd, Eugenio F. Fornasiero, Martin Holzenberger, Silvio O. Rizzoli and Inna Slutsky*

* Correspondence: Inna Slutsky, email: islutsky@tauex.tau.ac.il

This PDF file includes:

Figures S1 to S7

SI Methods

SI References

Supplementary Figures

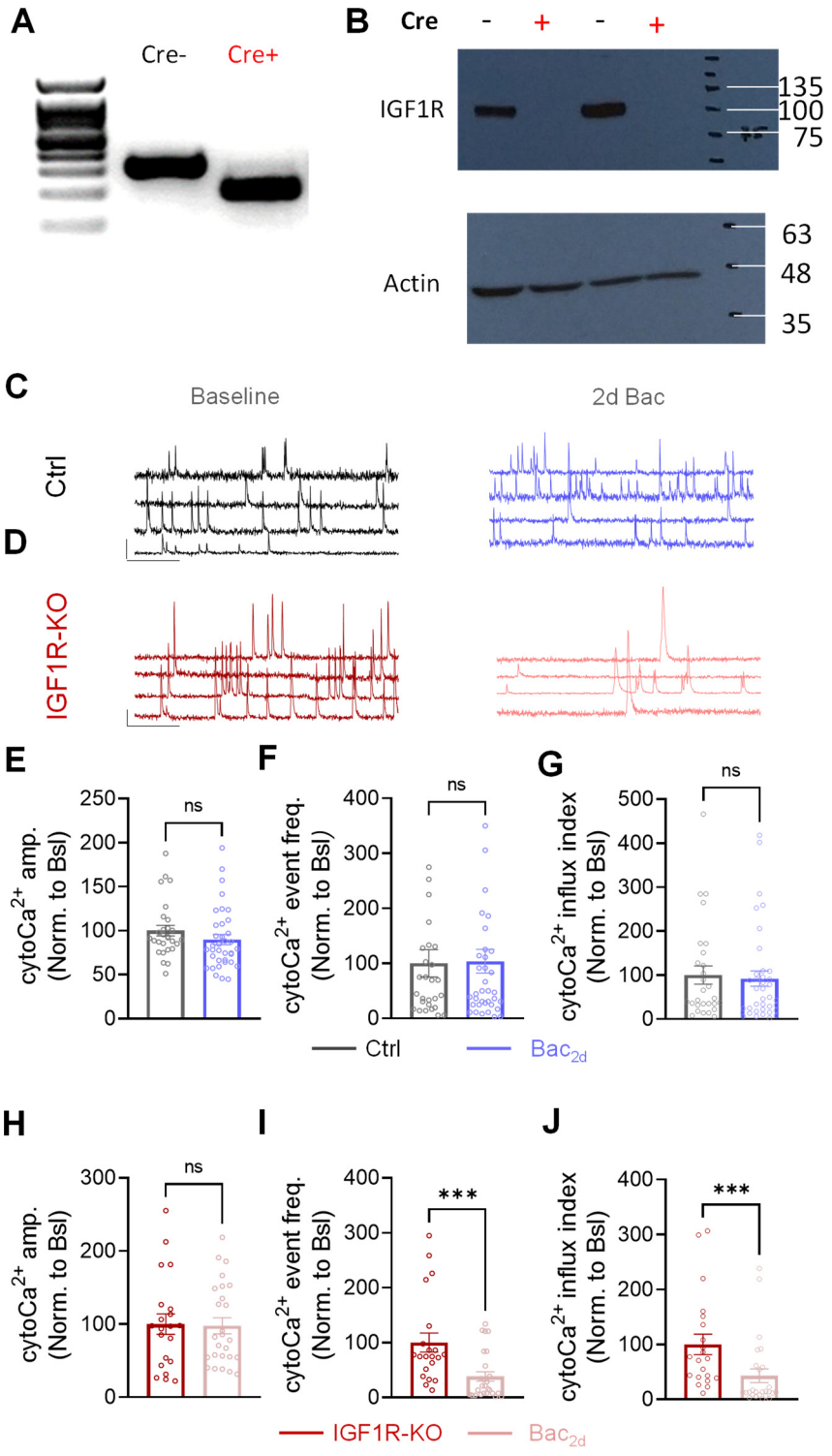

Figure S1. Deletion of IGF1R impairs homeostasis of cytoCa^{2+}. (*A-B*) Complete excision of IGF1R gene and elimination of IGF1R protein in Cre-infected IGF1R-fl/fl cultures. Cultures were collected to produce DNA and Protein. (*A*) IGF1R $^{flox/flox}$ vs. excised IGF1R genes in IGF1R-KO (Cre+) and Ctrl (Cre-) cultures. (*B*) Western-blot of IGF1R in IGF1R-KO and Ctrl cultures. (*C*) Example traces of cytoCa^{2+} of Ctrl excitatory neurons at baseline (*Left*) and following two days of Bac (*Right*). Scale bars: 20 sec, 0.5 $\Delta F/F$. (*D*) Example traces of cytoCa^{2+} of IGF1R-KO excitatory neurons at baseline (*Left*) and following Bac$_{2d}$ (*Right*). Scale bars: 20 sec, 0.5 $\Delta F/F$. (*E-G*) Bac$_{2d}$ did not affect mean cytoCa^{2+} amplitude (*P* =

0.07), frequency (P = 0.92) and cytoCa^{2+} influx index (mean amplitude*frequency, P = 0.57) in Ctrl neurons (n = 28 for Ctrl; n = 37 for Ctrl+Bac). (*H-J*) Effect of Bac_{2d} in IGF1R-KO neurons (n = 21 for IGF1R-KO, n = 26 for KO+Bac). (*H*) Mean cytoCa^{2+} amplitude in IGF1R-KO neurons was preserved following Bac_{2d} (P = 0.92). (*I*) Mean cytoCa^{2+} frequency in IGF1R-KO neurons was reduced to 38.3 ± 8.6% following Bac_{2d} (P = 0.0005). (*J*) The cytoCa^{2+} influx index in IGF1R-KO was reduced to 43.1 ± 12.3% following Bac_{2d} (P = 0.0005).

Mann-Whitney test (*E-J*). Error bars indicate SEM. ns, not significant, ***P < 0.001.

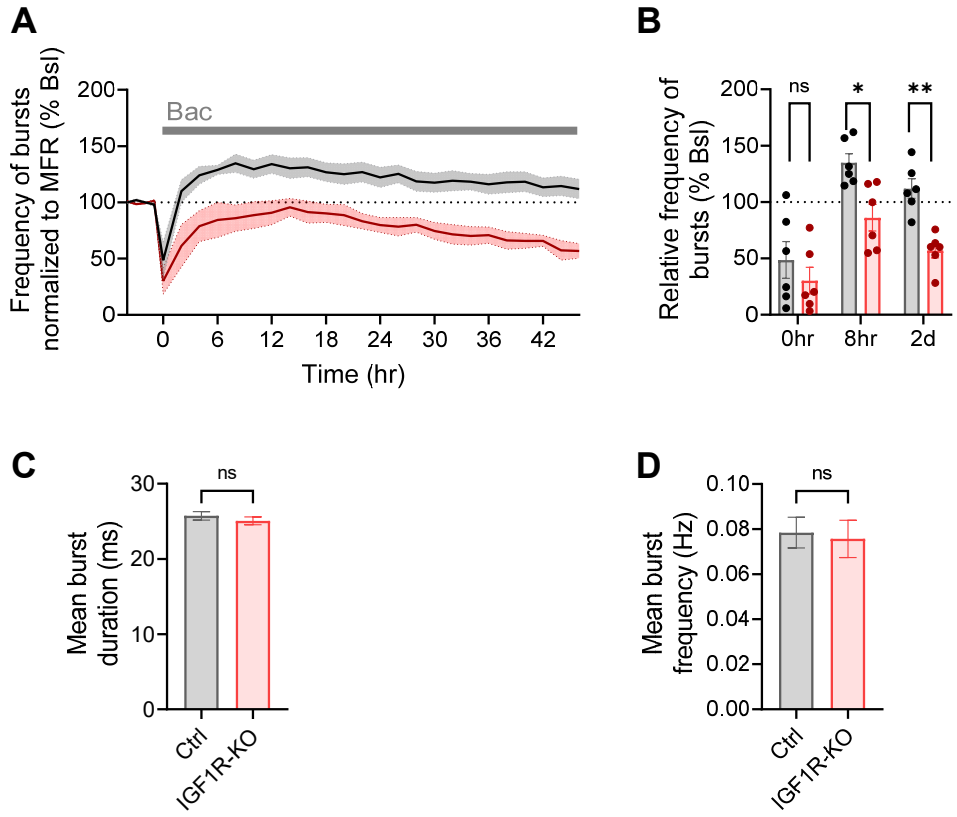

Figure S2. Effects of IGF1R-KO on spike pattern. (*A-B*) Homeostatic response of burst frequency, when normalized to MFR, is diminished in IGF1R-KOs. (N = 6 experiments, 519 units in Ctrl; N = 6, 347 units in IGF1R-KO). (*C-D*) No difference between Ctrl and IGF1R-KO in the mean burst duration (*C*, $P = 0.98$, 25.8 ± 0.6, n = 513 for Ctrl; 25.1 ± 0.5, n = 342 for IGF1R-KO) and in the frequency of bursts (*D*, $P = 0.56$, 0.078 ± 0.007, n = 519 for Ctrl; 0.076 ± 0.08, n = 347 for IGF1R-KO).

Two-way ANOVA with Sidak's multiple comparison test (*B*), Mann-Whitney test (*C,D*). Error bars indicate SEM. ns, not significant, $*P < 0.05$, $**P < 0.01$,$***P < 0.001$.

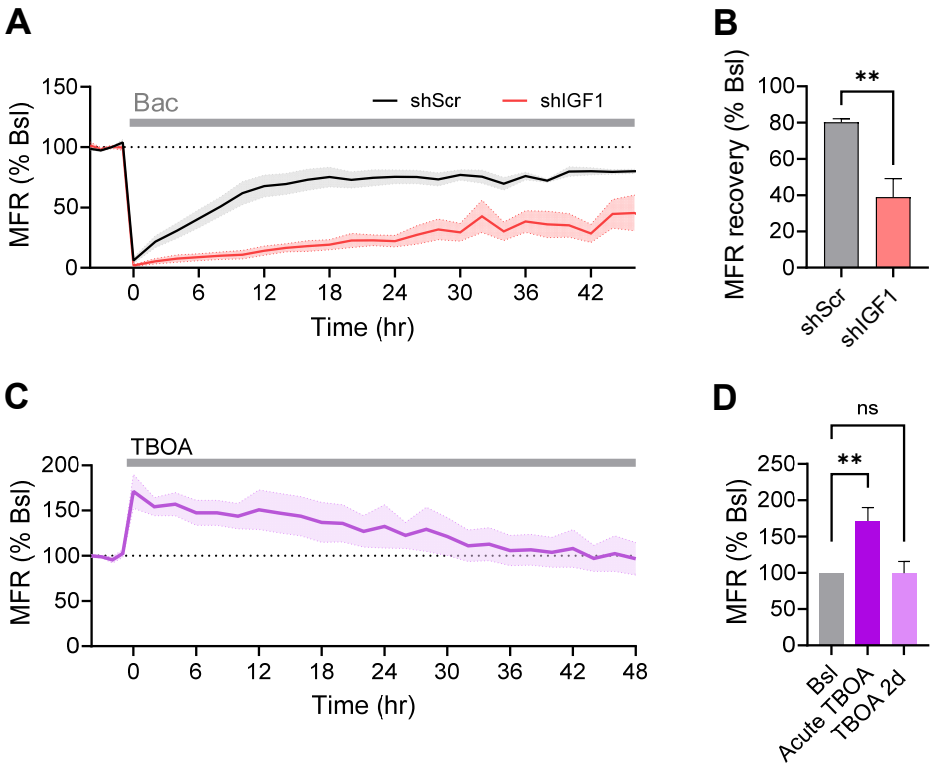

Figure S3. IGF1R-KOs are capable of maintaining MFR homeostasis when activity is increased pharmacologically. (*A*) Knock-down of IGF1 limits homeostatic response of MFR to inactivity. (shScr: N = 5 experiments, 304 channels; shIGF1: N = 5 experiments, 419 channels). (*B*) Reduced recovery of MFR to inactivity by KD of IGF1 .Each square represents an experiment (Same data as in *A*). (*C*) Mean and SEM of IGF1R-KO cultures, normalized to their baseline firing rate (6 experiments, 430 channels). (*D*) TBOA increased MFR to 171.3 ± 18.6%, followed by a homeostatic re-normalization back to baseline level ($P > 0.9999$, 99.48 ± 16.07 %, same data as in *C*).

Mann-Whitney test (*B*); Friedman's test with Dunn's correction for multiple comparisons (*D*). Error bars indicate SEM. ns, not significant, $^{**}P < 0.01$.

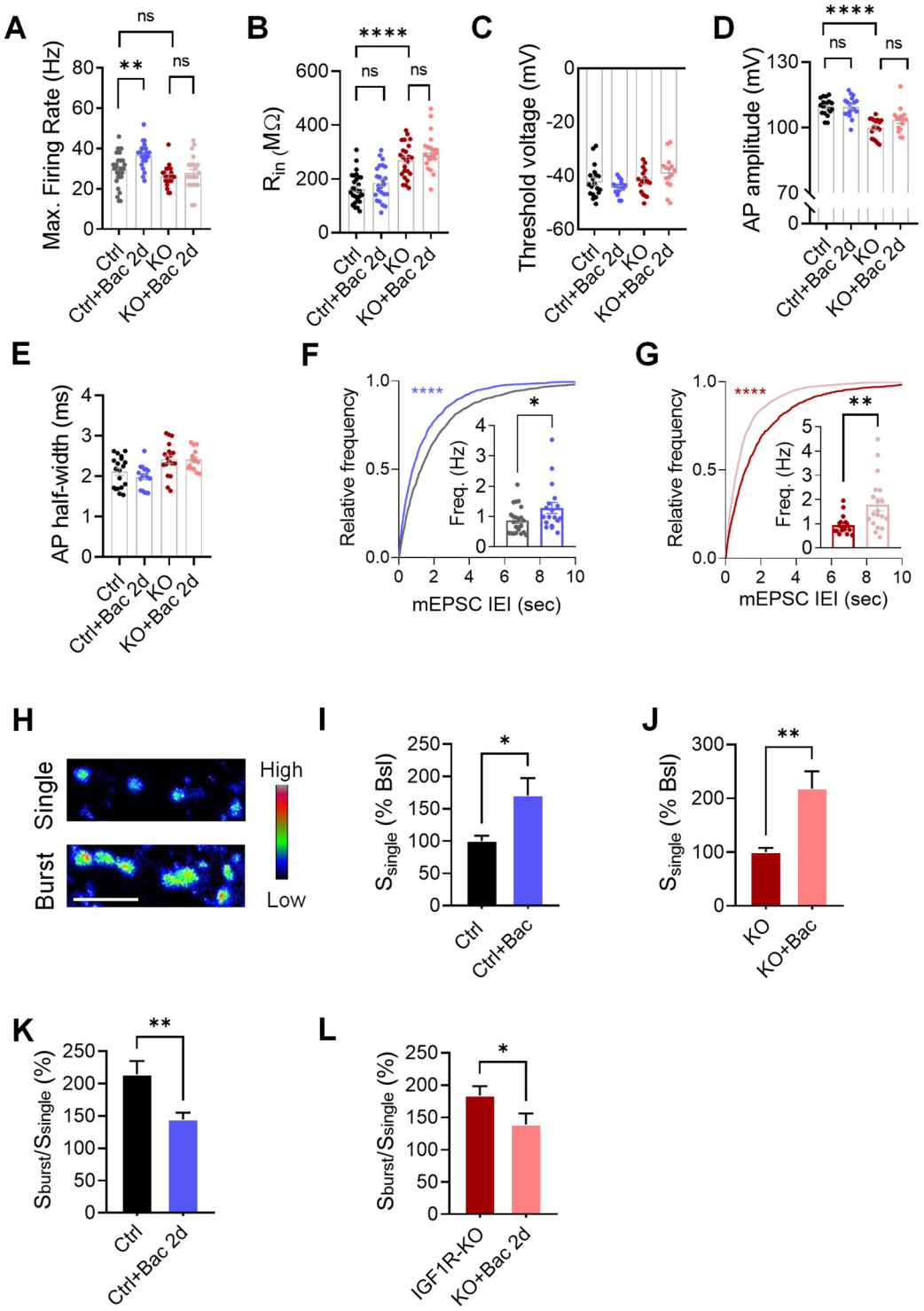

Figure S4. IGF1R-KO does not affect presynaptic functions, input resistance, and action potential threshold or waveform in response to baclofen. (*A*) Maximal firing rate is increased in Ctrl neurons following Bac_{2d} (29.4 ± 1.4 Hz, n = 29 for Ctrl; 36.6 ± 1.2 Hz, n = 24 for Ctrl+Bac), but does not change ($P > 0.9999$) in IGF1R-KO neurons (31.4 ± 2.6 Hz, n = 26 for IGF1R-KO; 27.8 ± 1.8 Hz, n = 22; for KO+Bac). (*B*) No change in input-resistance in neither Ctrl ($P = 0.864$) nor IGF1R-KO ($P > 0.9999$) neurons following Bac_{2d}. Increased input resistance in IGF1R-KO neurons compared to Ctrl (162.0 ± 10.3 MΩ, n = 29 for Ctrl; 184.8 ± 12.9 MΩ, n = 24 for Ctrl+Bac; 298.9 ± 24.4 MΩ, n = 26 for IGF1R-KO; 313.8 ± 20.6 MΩ, n = 23 for KO+Bac) (*C*) Threshold voltage does not change for any of the groups (42.19 ± 1.34 mV, n = 19 for Ctrl; -44.42 ± 0.61 mV, n = 18 for Ctrl+Bac; -42.11 ± 1.06 mV, n = 18 for

IGF1R-KO; -38.83 ± 1.625 mV, n = 15 for KO+Bac). (*D*) No change in action-potential amplitude in neither Ctrl ($P > 0.9999$) nor IGF1R-KO ($P = 0.3835$) neurons following Bac_{2d}. Decreased amplitude in IGF1R-KO neurons compared to Ctrl (109.5 ± 0.87 mV, n = 19 for Ctrl; 109.5 ± 1.083 mV, n = 18 for Ctrl+Bac; 99.77 ± 1.04 mV, n = 18 for IGF1R-KO; 103.4 ± 1.5 mV, n = 15 for KO+Bac). (*E*) No change in action-potential half-width between the groups (2.107 ± 0.087 ms, n = 19 for Ctrl; 1.978 ± 0.063 ms, n = 18 for Ctrl+Bac; 2.418±0.097 ms, n = 18 for IGF1R-KO; 2.406 ± 0.07 ms, n = 15 for KO+Bac). (*F*) Cumulative distribution of mEPSC inter-event intervals (IEIs) in Ctrl was shifted towards shorter IEIs following Bac_{2d} (n = 2063 events from 23 Ctrl neurons, n = 1885 events from 21 Ctrl+Bac neurons). *Inset*: On average, mean mEPSC frequency was increased following treatment (0.87 ± 0.09 Hz, n = 23 for Ctrl; 1.91 ± 0.49 Hz, n = 21 for Ctrl+Bac). (*G*) Cumulative distribution of mEPSP IEIs in IGF1R-KO was skewed towards shorter events following Bac_{2d} (n = 1351 events from 17 IGF1R-KO neurons, 1520 evets from 19 KO+Bac neurons). *Inset*: On average, mean mEPSC frequency was increased following Bac_{2d} (1.7 ± 0.4 Hz, n = 17 for IGF1R-KO; 3.17 ± 0.99 Hz, n = 19 for KO+Bac). (*H*) Representative images of FM-143 dye staining after 30 APs @ 1 Hz ('Single', *top*) and after 6 bursts (5 sec inter-burst interval) of 5APs @ 50Hz ('Burst', *bottom*). Scale bar: 3 µm. (*I,J*) Presynaptic strength (S_{single}) is increased following Bac_{2d} both in Ctrl cultures (*I*, 170.3 ± 27.1%, n = 15 for Ctrl; 144 ± 10.7%, n = 12 for Ctrl+Bac) and in IGF1R-KO cultures (*J*, 217.9 ± 32.3%, n = 16 for IGF1R-KO; n = 21 for KO+Bac). (*K,L*) Short-term presynaptic plasticity, quantified as S_{burst}/S_{single}, is reduced following Bac_{2d} both in Ctrl cultures (*K*, 214.5 ± 20.5%, n = 14 for Ctrl; 144 ± 10.7%, n = 12 for Ctrl+Bac) and in IGF1R-KO cultures (*L*, 184.0 ± 14.6%, n = 15 for IGF1R-KO; 138.8 ± 17.3%, n = 18 for KO+Bac).

Kruskal-Wallis test with Dunn's correction for multiple comparisons (*A-E*), Kolmogorov-Smirnov (*F,G*) and Mann-Whitney tests (*F,G,I,J*). Error bars indicate SEM. ns, not significant, $*P < 0.05$ $**P < 0.01$, $****P < 0.0001$.

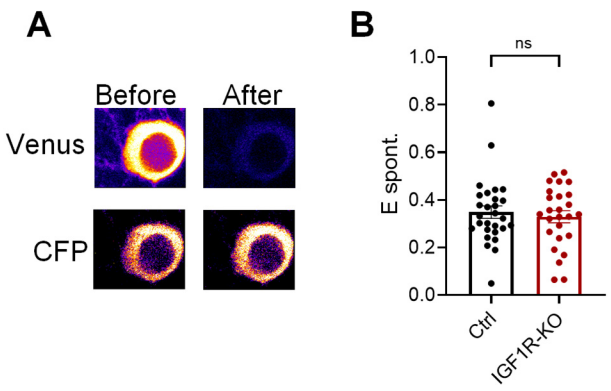

Figure S5. ATP level is unaltered in IGF1R-KO neurons (A) Representative neuron expressing cytosolic ATeam before (*left*) and after (*right*) acceptor photo-bleaching (*Top*). (B) (C) No difference (P = 0.925) in FRET efficiency of spontaneously active Ctrl (0.349 ± 0.026, n = 28) and IGF1R-KO (0.329 ± 0.025, n = 26) neurons.

Mann-Whitney test. Error bars indicate SEM. ns, not significant.

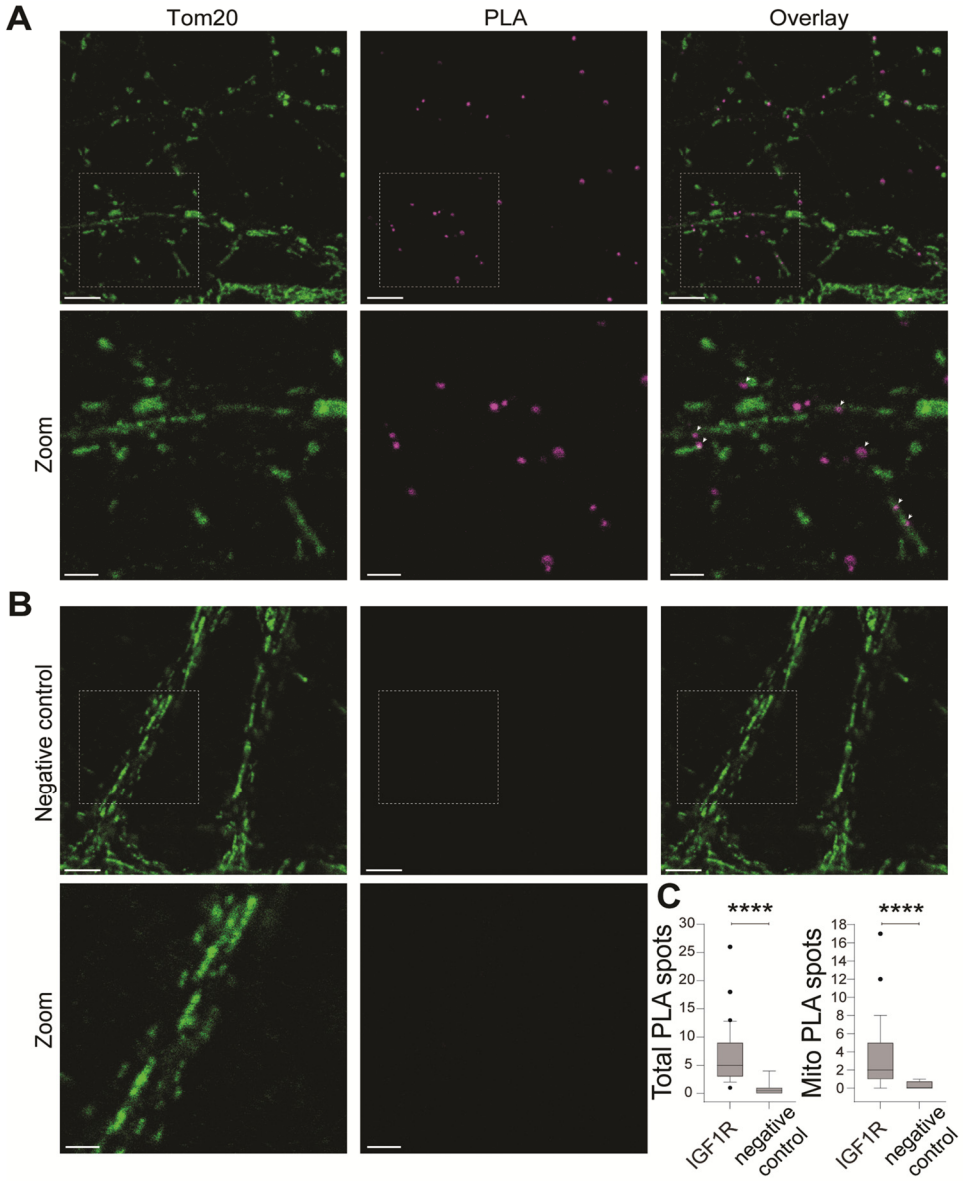

Figure S6. IGF1 is bound to IGF1R in neuronal mitochondria. IGF1R/IGF localize to mitochondria confirmed by proximity ligation assay (PLA). (*A*) Representative images of primary hippocampal neurons where the PLA reaction was performed in the presence of anti-IGF1R and anti-IGF1 antibodies. Only IGF1R/IGF1 in close proximity were revealed by PLA (*magenta*). For mitochondria colocalization analysis, neurons were coimmunostained for Tom20 (*green*) after the PLA reaction. Scale bars 5 µm. *Zoom*: higher magnification regions outlined in dash line in the upper panel. Arrowheads show clear colocalization of the IGF1R/IGF1 complex in mitochondria. Scale bars 2 µm. (*B*) As a negative control, the PLA reaction was performed only in the presence of IGF1R and coimmunostained for Tom20 (*green*). *Zoom*: higher magnification regions outlined in dash line in the upper panel. The amount of PLA positive spots was much lower. (*C*) Quantification shows ~5 PLA spots per image with ~2 localized in the mitochondria. Box plots represent 10, 25, 50, 75 and 90 percentiles.

Mann-Whitney test (*C*). ****$P < 0.0001$.

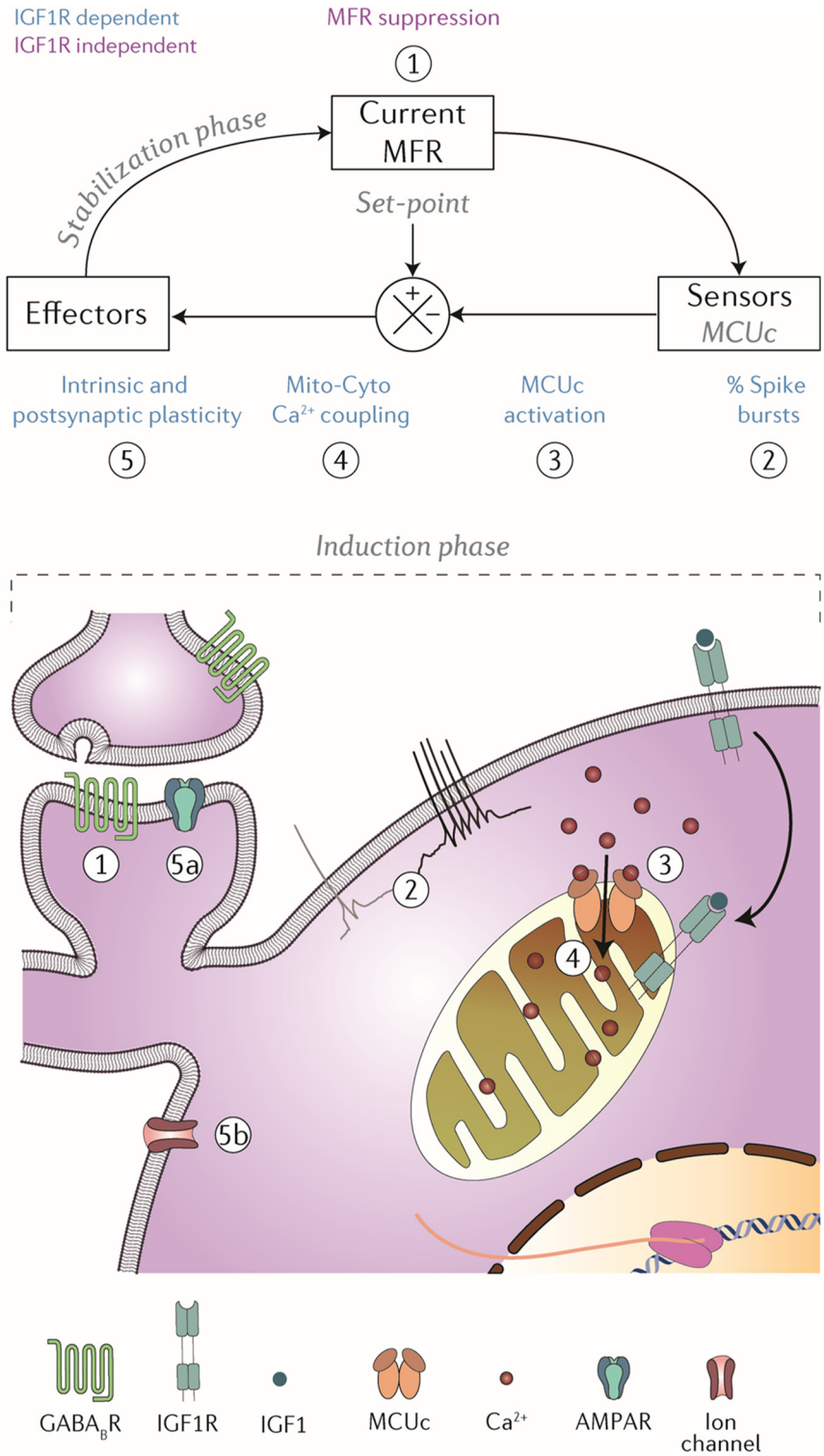

Figure S7. Model for IGF1R signalling in firing rate homeostasis. *Top*: diagram of MFR homeostatic plasticity using the framework of control theory. Titles in blue describe processes that require functional IGF1R. The processes are numbered according to the bottom scheme. *Bottom*: proposed model for the induction phase of upward MFR homeostasis. (1) $GABA_BR$ activation causes an acute decrease in MFR. (2) IGF1R is required for an increase in the fraction of spike bursts in response to the perturbation, leading to an increase in cytoCa^{2+} and subsequent (3) activation of MCUc. (4) IGF1R also maintains the coupling of mitochondria-to-cytosol Ca^{2+} coupling. (5) As a result, IGF1R enables the induction of intrinsic and postsynaptic homeostatic plasticity that underlies MFR recovery to a set-point level.

SI Methods

Primary hippocampal culture preparation

Hippocampi were dissected from IGF1R$^{fl/fl}$ (1) pups (both sexes) at P0-1in ice cold Leibovitz L-15 medium. Tissue was washed 3 times with Hank's balance salt solution (HBSS). Chemical dissociation of cells was done using digestion solution (137 mM NaCl, 5 mM KCl, 7 mM Na_2HPO_4, 25 mM HEPES, 2 mg/mL trypsin, 0.5 mg/mL DNase) for 10 min in an incubator. Solution was replaced by HBSS supplemented with 20% FBS to inactivate trypsin and once again with only HBSS. Cells were then mechanically dissociated in HBSS supplemented with 13 mM $MgSO_4$ and 0.5 mg/mL DNase by titration with fire-polished pipettes of decreasing diameter. Sedimentation of cells was accomplished by centrifugation at 1000 r*cf* for 10 min at 4°C. After the removal of the supernatant, cells were re-suspended with plating medium (MEM supplemented with 10% FBS, 32.7 mM glucose, 25 mg/mL insulin, 2 mM Glutamax, 0.1 mg/mL transferrin, 0.1% SM1) and then plated on matrigel-coated glass coverslips, glass-bottom 24-wells or MEA plates. Half of the serum medium was replaced with feeding medium the day after (MEM supplemented with 32.7 mM glucose, 2 mM Glutamax, 3 µM ARA-C, 0.1 mg/mL transferrin, 2% SM1). Afterwards, half of the medium was replaced with fresh feeding medium every 3-4 days for three additional times. For all electrophysiology and live cell imaging, cultures were infected at 5-6 days *in-vitro* (DIV) with Cre+ or Cre- AAVs, shScr or shIGF1 AAVs, and with MCUc (MCU, MICU1 and MICU3) or mtIGF1R on DIV 8&9 (MCU and MICU1 on day 8, and MICU3 on the next day). The experiments were performed in cultures after 14 – 21 DIV.

Plasmids

For CBAP-Cre-P2a-Cerulean and CBAP-P2a-Cerulean, cDNA encoding for Cre was obtained from K.Villa. AAV2-CBAP plasmid was obtained from Daniel Gitler (BGU, Israel). Cre-P2a-Cerulean or P2a-Cerulean were fused in frame by PCR and cloned into AAV2-CBAP. AAV-hSynI-jRGECO1a was prepared by inserting jRGECO1a (pGP-CMV-NES-jRGECO1a, Addgene plasmid # 61563) into AAV2-hSynI-AT1.03 NL (gift from Daniel Gitler), replacing AT1.03 NL. For AAV2-CaMII2a-4mtGCaMP8m, 4mt fragment (synthesized by GenScript) was in frame fused to jGCaMP8m (Addgene #162372) and cloned into Addgene plasmid #51086, replacing GCaMP6s-p2A-nls_dTomato. Construction of AAV-hSynI-2mt-mCherry was described in (2). Mouse MCU (NM_001033259.4) and MICU1 (NM_144822.3) were synthesized by GenScript. Mouse MICU3 (NM_030110.2) was synthesized by Genwiz. P2a-mCherry was inserted into AAV2-CBAP, then MCU, MICU1 or MICU3 were cloned in frame with P2a-mCherry. For shRNA-mediated knockdown of mouse IGF-1 or control vector, the whole

cassette U6-shIGF1-hSyn-mCherry from pLL3.7 (34) or U6-shScrambled-hSyn-mCherry were cloned into AAV2-hSyn1, replacing the pre-existing promoter. For 4mtIGF1R-mTagBFP2: cDNA encoding to IGF1R was in frame fused to 4mt (synthesized by GenScript) and mTagBFP2 (p773, ETH, Switzerland) by PCR. The obtained 4mtIGF1R mTagBFP2 was inserted into AAV2-CBAP plasmid, giving AAV2-CBAP-4mtIGF1R-mTagBFP2 (called mitoIGF1R).

Electrophysiology

MEA data acquisition and analysis

Cells were grown on MEA plates [Multi Channel Systems (MCS), 120MEA200/30iR-Ti] containing 120 titanium nitride (TiN) electrodes with 4 internal reference electrodes. Each electrode's diameter is 30 μm and they are spaced on a 12X12 grid (24 spaces in the 4 corners did not contain electrodes), spaced 200 μm apart. Data was recorded by either a MEA2100-System (MCS) with a chamber that maintained 37°C and 5% CO2, or a MEA1200-mini-system (MCS) that was constantly placed inside an incubator. Raw data was collected at 10 kHz, with a hardware high-pass filter of 1 Hz and an upper cut off of 3.3 kHz for the MEA2100-system and 3.5 kHz for the MEA2100-mini-system.

Using MCS data analyzer software offline, raw data were filtered by a Butterworth 2nd order high-pass filter at 200 Hz. Spikes were then detected by a fixed threshold of 6 SD. To reduce processing and analysis time, each hour was represented by 20 min of recording, which was previously shown to reliably represent the MFR of the full hour (3). For spike sorting, Plexon offline-sorter V3 (Plexon inc. USA) was used. Principle component analysis was carried out on a 2-D or 3-D space. Distinct clusters were manually selected, and an automatic template sorting was done on the rest. Clusters' stability throughout the recording was manually inspected. Only clusters that fulfilled the following requirements were considered units and used for the analysis: (1) No spikes in refractory periods. (2) The clusters were well defined during the entire experiment. (3) There were no sudden jumps in cluster location on PC axes. The rest of the analysis was carried out using a custom-written MATLAB (Mathworks) script as described in (3). For detection of bursts at the single-unit level, bursts were defined as 2 or more spikes at a minimum of 20 Hz based on the code we previously published (3). Our previous analysis shows that the results are robust over a wide range of burst parameters (3).

Patch clamp whole-cell recordings and analysis

Experiments were performed at room temperature in a RC-26G recording chamber (Warner instrument LCC, USA) on the stage of FV300 inverted confocal microscope (Olympus, Japan) using a Multiclamp 700B amplifier and a Digidata 1440A digitizer (Molecular devices, LLC, USA). All experiments were

carried out using extracellular Tyrode solution containing (in mM): NaCl, 145; KCl, 3; glucose, 15; HEPES, 10; $MgCl_2$, 1.2; $CaCl_2$, 1.2; pH adjusted to 7.4 with NaOH, and intracellular solution containing (in mM): K-gluconate 120; KCl 10; HEPESs 10; Na-phosphocreatine 10; ATP-Na_2 4; GTP-Na 0.3; $MgCl_2$ 0.5. Intracellular solution was supplemented with 20 µM Alexa fluor 488 for dendritic spines imaging. For intrinsic excitability, synaptic blockers were used (in µM): 10 CNQX, 50 AP-5, and 10 gabazine. For mEPSCs recordings, tetrodotoxin (1 µM), AP-5 (50 µM), and gabazine (10 µM) were added to Tyrode's solution. Intrinsic excitability protocols: small DC current was injected in current-clamp mode to maintain membrane potential at -65 mV. For I-F curve: positive currents from 40 to 600 pA were injected in 40 pA increments for 500 ms. Input resistance (R_{in}) was measured by calculating the slope of the voltage change in response to increasing current injections from -80 to +20 mV in 20 mV increments. For single AP measurements, 2 ms currents were injected at 40 pA increments. For mEPSCs recordings, neurons were voltage-clamped at -65 mV. Neurons were excluded from the analysis if no dendritic spines were observed, serial resistance was > 15 MΩ, serial resistance changed by >20% during recording, or if R_{in} was < 75 MΩ. Signals were recorded at 10 kHz, and low-pass filtered with Bessel filter 2 kHz. Electrophysiological data were analyzed using pClamp (Molecular Devices LLC, USA) and MiniAnalysis (Synaptosoft, Decatur, Georgia, USA) for mEPSC. For distributions of mEPSCs, 90 first events were taken from each neuron to prevent over-representation of high-frequency neurons.

Confocal live cell imaging

Evoked cytosolic and mitochondrial calcium imaging in neuronal soma

Experiments were performed on a FV-1000 (Olympus, Japan) system using a QR/RC-47FSLP chamber with a TC-324C temperature controller (Warner Instruments LLC, USA) at 33-34°C. In-chamber temperature stability was verified between coverslips with a Newtron TM-5005 thermometer. Coverslips were placed in Tyrode's solution that contained (in mM): NaCl, 145; KCl, 3; glucose, 15; HEPES, 10; $MgCl_2$, 1.2; $CaCl_2$, 1.2; pH adjusted to 7.4 with NaOH at 34°C. Synaptic blockers were used to prevent recurrent activity from stimulation (in µM): 10 CNQX, 50 AP-5. Cultures were infected with AAV1/2-hSyn-jRGECO1a and AAV1/2-CaMKIIα-4mt-GCaMP8m, so that only excitatory neurons expressed both Ca^{+2} sensors. Only cells with mitochondrial response to a 10-stimuli burst at 50 Hz were considered. Infection with AAV1/2-CBAP-Cre-Cerulean or AAV1/2-CBAP-Cerulean was verified with a 440 nm laser. Imaging was done with a 60X lens and X1.5 digital magnification at ~12.5 frames per second with 488 nm and 561 nm lasers, and emission spectra of 505 – 540 nm and 575 – 675 nm for GCaMP8m and jRGECO1a, respectively. Field stimulation was given using a SIU-102 stimulation unit (Warner Instruments LLC, USA) connected to an Axon Digidata 1440A digitizer (Molecular devices, LLC, USA).

Each imaged neuron was stimulated by a single stimulus and bursts of 3, 5 and 10 stimuli at 50 Hz. Some neurons had more than one clear response to 3, 5 or 10 stimuli and thus excluded from analysis. Analysis were done using ImageJ.

Spontaneous cytosolic calcium in neuronal soma

Experiments were performed on a FV-1000 (Olympus, Japan) system. Cultures were plated on #0 glass bottom 24 well (Cellvis, USA) and imaged in a heated (34-35°C) Stage-Top Incubator System TC, connected to a CU-501 temperature controller and a humidifier delivering 5% CO2 air (Live Cell Instruments, Republic of Korea). Imaging parameters were the same as for the evoked imaging. Each neuron was recorded 3 times for 3 min, with a 3-min interval to prevent bleaching and phototoxicity. Analysis was done using ImageJ (for extraction of florescence intensity over time) and a custom-written MATLAB script (for dF/F calculation and event identification and quantification).

FRET efficiency imaging

Primary hippocampal cultures were infected on DIV5-6 by AAV1/2 encoding Cre-P2a-mCherry sequences or P2a-mCherry sequence. Experiments were performed on a FV-1000 (Olympus, Japan) system at room temperature. Some coverslips were placed in Tyrode's solution that contained (in mM): NaCl, 145; KCl, 3; glucose, 15; HEPES, 10; $MgCl_2$, 1.2; $CaCl_2$, 1.2; pH adjusted to 7.4 with NaOH. Others were placed in their own media, in a heated (34-35°C) Stage-Top Incubator System TC, connected to a CU-501 temperature controller and a humidifier delivering 5% CO_2 air (Live Cell Instruments, Republic of Korea). The results were similar for both conditions so they were pooled. Infection of neurons with AAV1/2-CBAP-Cre-mCherry or AAV1/2-CBAP- mCherry was verified with a 561 nm laser. Images of neuronal soma were taken before and after acceptor (cpmVen) photobleaching. Donor (mseCFP) was excited with a 440 nm laser, and emission was measured at [460-500] nm before (I_{DA}) and after (I_D) photobleaching. Bleaching was accomplished using a 514 nm laser. Images of acceptor were taken before and after bleaching at [530-600] nm, to asses bleaching level: neurons with less than 85% reduction in fluorescence were excluded. FRET efficiency was calculated as [I_{DA}/ I_D].

FM-based imaging

Activity-dependent FM1-43 (10 μM) styryl dye was used to estimate basal synaptic vesicle recycling and short-term plasticity using protocols described previously (4). Briefly, APs in neurons were initiated by field stimulation during dye loading, and the terminals, after undergoing vesicle exocytosis coupled to endocytosis, were stained by FM1-43 10 μM FM1-43 has been present 5 sec before and 20 sec after the electrical stimulation. During FM loading and unloading, kynurenic acid (0.5 mM) was added to Tyrode

solution to prevent recurrent activity through blockage of excitatory postsynaptic responses during loading and unloading. After dye loading, external dye was washed away in Ca^{2+}-free solution containing ADVASEP-7 (0.1 mM; Sigma). To confirm that the fluorescent spots corresponded to release sites, we evoked 600 APs @ 5 Hz during the unloading step to obtain release of dye–filled vesicles. The total amount of releasable fluorescence at each bouton (ΔF) was calculated from the difference between fluorescence after loading and after unloading ($\Delta F = F_{loading} - F_{unloading}$). The total presynaptic strength during low-frequency stimulation (loading of 30 APs @ 1 Hz) has been calculated as $S_{single} = \Delta F \times D$, whereas D is the number of FM-(+) terminals per FM image. To determine the total presynaptic strength during burst patterns (Sburst), 30 APs have been delivered by bursts consisting of 5 APs @ 50 Hz, inter-burst-intervals of 5 s. To determine the sign and magnitude of short-term plasticity, we calculated the Sburst / Ssingle ratio over the same image area. Image analysis was carried out using ImageJ.

STED microscopy

Immunostaining was carried out based on standard protocols. Cultured hippocampal neurons (prepared exactly as described (5)) were fixed with 4% PFA in PBS for 30 min, followed by quenching with 100 mM glycine in PBS for 15 min, before being permeabilized and blocked using a blocking buffer prepared with 2% BSA (Sigma, 9048-46-8) in PBS added to 0.1% TritonX-100 (Merck, Kenilworth, NJ, USA). Next, the cells were incubated overnight with primary antibodies diluted in blocking reagent, at 4 °C. The neurons were then incubated with the appropriate secondary antibody (1:400) for 60 min at room temperature. The coverslips were mounted using Mowiol (Merck Millipore, Kenilworth, NJ, USA). The following primary antibodies were used: MICU1 rabbit polyclonal (1:100; Sigma), MICU2 rabbit polyclonal (1:50; Sigma), MICU3 rabbit polyclonal (1:150; Sigma), MCU rabbit polyclonal (1:100; Sigma), TOM20 mouse monoclonal (1:100; Sigma), and IGF1Rβ mouse monoclonal (1:100; Invitrogen, 194Q13). The applied secondary antibodies were anti-mouse STAR580 and anti-rabbit STAR635P purchased from Abberior GmbH, Göttingen, Germany.

Epifluorescence images (Fig. 6C,D) were obtained by means of an IX83 inverted microscope (Olympus). STED imaging (Fig. 6E,E`) was captured using a STED Abberior microscope, Göttingen, Germany. Excitation lines of 640 nm and 561 nm were adopted for exciting Star653P (MCUc subunits) and Star580 (TOM20 and IGF1R). For STED excitation, pulsed lasers were set at 640 nm and 580 nm. STED depletion was implemented via 775 nm depletion laser and the images were acquired at 20 nm pixel size.

Proximity ligation assay (PLA)

Primary hippocampal neurons were cultured and fixed as described above. PLA was carried out using Duolink™ In Situ Orange Starterkit Mouse/Rabbit (DUO92102-1KT, Merck) according to the Duolink® PLA Fluorescence Protocol. Primary hippocampal neurons were immunostained with anti-mouse IGF1Rβ (1:100, Invitrogen, 194Q13) and anti-rabbit IGF1 (1:100, abcam, ab9572) primary antibodies. After the PLA reaction, neurons were immunostained with the anti-rabbit Tom20 polyclonal antibody directly conjugated to CoraLite®488 (1:100, CL488-11802, Proteintech). Coverslips were embedded with Duolink® In Situ Mounting Medium with DAPI and sealed to avoid leaking. Imaging was performed in the confocal mode using an Abberior microscope (Göttingen, Germany). The CoraLite®488 fluorophore was excited using a 488 nm laser line and the PLA fluorophore was excited using a 561 nm laser line. Images were acquired in 40 × 40 µm size with a pixel size of 40 × 40 nm and 10µs pixel dwell time.

Brain and free mitochondria purification

Brain lysates and free mitochondria were isolated as previously described (6) form 5-month-old C57BL/6Rj with minor modifications. Briefly, upon rapid brain extraction, the forebrain was dissected, cleaned from meninges and washed in isolation buffer, to remove blood. Buffers were prepared exactly as described in (6). The tissue was then homogenized with method A (using a dunce homogenizer) with a two-step approach, as detailed in (6). The homogenate obtained was used for the "total brain lysate" samples. After the two centrifugations at 1,300 g at 4°C, the supernatants were further centrifuged at 21,000 g at 4°C for 10 min while preparing the Percoll (GE Healthcare, cat. no. 17089101) gradients. The pellet was resuspended in 15% Percoll solution at 4°C by gentle pipetting. This resuspended crude mitochondrial fraction was layered gently on the Percoll gradient and centrifuged at 30,700 g at 4°C for 5 min. After centrifugation, the lower band that contains the highly enriched mitochondrial fraction at the interface between the 23% and 40% Percoll layers (termed band 3) was collected, further concentrated by a 16,700g 10 min centrifugation at 4°C. These mitochondria were named "free mitochondria" and were used for further analyses.

Western blotting

Protein concentration was measured with the Pierce™ BCA Protein Assay Kit (Thermo Fisher Scientific, 23225) following the manufacturer's guidelines. Samples of identical protein concentrations were run in parallel gels containing 10% or 20% polyacrylamide (Roth A124.2), and bands were separated with SDS-PAGE. Gels were then transferred to nitrocellulose blotting membranes (Amersham Protran Premium 10600003) for 2 hours at 1.25 A. Membranes were blocked in 5% skim milk powder (Sucofin) for 1h at

RT in TBS-Tween20 buffer (20 mM Tris; 150 mM NaCl; 0.1% Tween 20). Membranes were incubated with the respective primary antibodies diluted in the blocking buffer overnight at 4°C. Membranes were rinsed for 30 min in TBS-Tween20 and incubated for 1 h at room temperature with the corresponding secondary LICOR antibodies (see antibody list for details) and finally washed in TBS-Tween20 for 30 min. As a control for loading reproducibility, the blots were probed with an anti-GADPH antibody and revealed with the respective secondary antibody. After secondary antibody incubation, the fluorescent images of the nitrocellulose membranes were acquired with a LICOR Odyssey CLX-2088 imaging system. To cleave all proteins from the outer membranes of the organelles in the brain lysates and the free mitochondria, the samples were divided into 2 groups: one treated with trypsin (+ trypsin; Thermofisher Gibco 25300-054) and an untreated group (- trypsin). Primary antibodies: mouse anti-IGF-1Rβ antibody (1:500; Invitrogen, 194Q13); mouse anti-GAPDH (1:5000; Proteintech 60004-1-Ig), mouse anti-Cox4-1 (1:500; custom-made, identifier PRAB1522, a generous gift from Dr. Sven Dennerlein (University Medical Center Göttingen, Germany) characterized in (7). Secondary antibodies: donkey anti-mouse IgG antibody conjugated to IRDye 800 CW (1:5000; Li-Cor 926-32212); donkey anti-rabbit IgG antibody conjugated to IRDye 680 RD (1:5000; Li-Cor 925-68072).

Real-time PCR

RNA was extracted using the TRI Reagent, according to the manufacturer's instructions (Sigma-Aldrich). Equal amount of mRNA was reverse-transcribed to cDNA with Superscript III reverse transcriptase (Invitrogen, cat. No: 18080-051). Real-time qPCR was performed with Sybr mix (Applied Biosystems). Reactions were run in triplicate in a StepOnePlus real-time PCR system (Applied Biosystems). mRNA abundance was calculated by means of the comparative cycle threshold (Ct) method following the manufacturer's guidelines. mRNA expression level was normalized to the average expression of B*2m* and *Polr2a*.

B2m	5' GTCTTTCTATATCCTGGCTCACACTG- Forward 5' CATGTCTCGATCCCAGTAGACG- Reverse
Polr2a	5'ATCAAGAGAGTGCAGTTCGGAGTC-Forward 5'ATCAAGAGAGTGCAGTTCGGAGTC-Reverse
MCU	5' GTTAGAGGACCTCAAGCAGCA – Forward 5' CCTCTTCTCTGCTTTTCTGCTAA- Reverse

MICU1	5’ AATGACGTGGACACTGCACTA- Forward 5’ CCACTTGCTGCATGGTCA- Reverse
MICU2	5’ GGATGGGAATGAGATGATCG- Forward 5’ TTGAAGCCATCTTGTTTACTTATGA- Reverse
MICU3	5’ CCAAATTTGCTAAAACGTGGA- Forward 5’ AAAGCTTTGATGATCCCTTCC- Reverse

AAV vector production

AAV vector production was carried out in 293T cells. Cells were transfected 24 h after seeding with helper plasmids encoding AAV rep, cap and plasmid for the rAAV cassette expressing the relevant DNA. Cells were harvested 72 h after transfection, cells pellet was resuspended in lysis solution (150 mM NaCl, 50 mM Tris-HCl, pH 8.5), 1mL of lysis buffer per 150 mm dish. Cells were lysed by a few freeze-thaw cycles. The obtained crude lysate was treated with 50 U benzonase (Sigma, E1014) per 1 mL of lysate at 37°C for 1.5 h to degrade genomic DNA. Cell debris were pelleted by centrifugation at 3000*g* for 15 min 4°C. Supernatant contains crude virus was filtered through a 0.45 um filter and stored at 4°C.

Western Blot

Primary hippocampal cultures were infected on DIV5-6 by AAVs encoding cre-P2a-mCherry sequences (+Cre) or P2a-mCherry sequence (-Cre). Lysates of equal number of cells (~500k) were separated by SDS-PAGE, transferred to nitrocellulose, blocked with 5% skim milk powder (Difco # 232100) and incubated ON with anti-IGF-1R antibody (#3027 CST), followed by anti-rabbit-HRP secondary antibody (#11-035-044 Jackson ImmunoResearch). To normalize the signal, the blot was re-probed with anti-actin antibody (Sigma), followed by anti-mouse-HRP secondary antibody (#115-035-146 Jackson ImmunoResearch).

Knockout validation at the level of genomic DNA

Primary hippocampal cultures were infected on DIV5-6 by AAVs encoding cre-P2a-mCherry sequences (+Cre) or P2a-mCherry sequence (-Cre). Cells were collected and lysed, and DNA was purified using the MasterPure™ DNA&RNA Complete purification kit according to the company’s manual (Cat.

MC85200 epicentre). DNA was probed with primers for the excised and not excised version of the floxed exon3 of the IGF1R gene with the following primers:

RloxYNex	5'- CCA TGG GTG TTA AAT GTT AAT GGC -3'
RloxYNmt2	5'- ATC TTG GAG TGG TGG GTC TGT TTC -3'
RloxYNvl	5'- ATG AAT GCT GGT GAG GGT TGT CTT -3'

References

1. Holzenberger M*, et al.* (2000) A targeted partial invalidation of the insulin-like growth factor I receptor gene in mice causes a postnatal growth deficit. 141(7):2557-2566.
2. Styr B*, et al.* (2019) Mitochondrial Regulation of the Hippocampal Firing Rate Set Point and Seizure Susceptibility. *Neuron* 102(5):1009-1024.e1008.
3. Slomowitz E*, et al.* (2015) Interplay between population firing stability and single neuron dynamics in hippocampal networks. *eLife* 4.
4. Abramov E*, et al.* (2009) Amyloid-[beta] as a positive endogenous regulator of release probability at hippocampal synapses. *Nat Neurosci* 12(12):1567-1576.
5. Jähne S*, et al.* (2021) Presynaptic activity and protein turnover are correlated at the single-synapse level. 34(11):108841.
6. Sims NR & Anderson MFJNp (2008) Isolation of mitochondria from rat brain using Percoll density gradient centrifugation. 3(7):1228-1239.
7. Richter-Dennerlein R*, et al.* (2016) Mitochondrial protein synthesis adapts to influx of nuclear-encoded protein. 167(2):471-483. e410.